Effects of Natural Chitosan as Biopolymer Coupling Agent on the Pyrolysis Kinetics of Wood Flour/ Polyvinyl Chloride Composites

Kaimeng Xu,[a] Taian Chen,[a,]* Zhifeng Zheng,[a,]* Suyong Huang,[a] Kaifu Li,[b] and Tuhua Zhong [c]

The thermal degradation behavior and pyrolysis kinetic models of wood flour (WF)/PVC composites before and after adding chitosan were studied using thermogravimetry (TGA) and nine common kinetic model functions ($f(\alpha)$). The results indicated that the thermal degradation temperature of WF/PVC composites was delayed to a higher value after adding chitosan. The first-order reaction order (L1) model and second-order reaction order (L2) model were found to be the best reaction order functions for the description of mass loss kinetics of WF/PVC without chitosan during the first and second stages. Two L2 models were suitable for both degradation stages of WF/CS/PVC. Activation energy (E) and frequency factor (A) for WF/PVC and WF/CS/PVC corresponded to 26.05 kJ·mol^{-1}, 4.08×10^{3} s^{-1}, and 40.89 kJ·mol^{-1}, 2.11×10^{10} s^{-1} at the first degradation stage, respectively, and 97.83 kJ·mol^{-1}, 1.11×10^{7} s^{-1} and 92.88 kJ·mol^{-1}, 1.56×10^{11} s^{-1} at the second degradation stage.

Keywords: Chitosan; Wood flour; PVC; Pyrolysis kinetic model

*Contact information: a: University Key Laboratory of Biomass Chemical Refinery & Synthesis of Yunnan Province, College of Material Engineering, Southwest Forestry University, Kunming 650224, P.R. China; b: Department of Forestry, South China Agricultural University, Guangzhou 510642, P.R. China; c: Division of Forestry and Natural Resources, West Virginia University, Morgantown, WV 26505, USA; * Corresponding authors: chentaian6868@163.com; zhengzhifeng666@163.com*

INTRODUCTION

The decline in forestry resources and a rise in awareness of environmental protection have greatly kindled the fast development of emerging alternative materials. Wood plastic composites (WPC) are one of many potential novel materials to replace solid wood and conventional wood-based composites, such as particle board (PB), medium density fiberboard (MDF), and plywood (Lu *et al*. 2008; Fabiyi *et al*. 2009; Yue *et al*. 2011; Segerholm *et al*. 2012; Cavdar *et al*. 2014). Wood flour/polyvinyl chloride (WF/PVC) composites are a primary subset of WPC, which had great growth in different applications in the global market in the last few decades due to their unique wood-like appearance, the fact that they are easy to paint, their ability to readily form foams, their excellent resistance to biodegradation, and low cost of maintenance (Jiang and Kamdem 2004; Muller *et al*. 2012; Kositchaiyong *et al*. 2013; Xu *et al*. 2013; Kositchaiyong *et al*. 2014).

Interfacial bonding and thermal stability are currently two difficult problems that impede the use of WF/PVC in more fields. Compared to polyolefin resins, such as polyethylene (PE) and polypropylene (PP), PVC contains additional carbon-chlorine (C-Cl) bonds in its molecular structure, resulting in a special molecular chain of polarity, which has a significant effect on interfacial bonding of PVC and wood flour. With respect to thermal stability, it is well known that hydrogen chloride (HCl) is eliminated from PVC during the heating process. As for WF/PVC, the initial dehydrochlorination of the PVC macromolecular chains would be accelerated owing to the acidic products in wood flour (McNeill *et al*. 1995), which would lead to inferior organoleptic properties (odor and color) and deterioration of physical-mechanical properties (Fang *et al*. 2012).

In previous studies by the authors it was concluded that natural chitosan is an excellent biopolymer coupling agent and anti-bacterial agent to promote interfacial adhesion and added value of WF/PVC when being added in the optimum amount (Xu *et al*. 2014a). Meanwhile, due to the effects of alkalescence and the coupling function from the -NH_2 groups in CS molecular chains, it was also deduced that the autocatalytic effect of HCl on continuous dehydrochlorination of PVC macromolecular chains was partly crippled due to the adsorption and acid-base neutralization by CS (Karayildirim *et al*. 2006; Xu *et al*. 2014b).

The pyrolysis kinetic model of polymeric materials is acknowledged as an accurate prediction of the flammability and fire hazard properties, especially for polymers and wood fibers that are very sensitive to flame (Sain *et al*. 2004; Snegireva *et al*. 2012; Czégény *et al*. 2015). Therefore, it is also of great importance in understanding the mechanism of thermal degradation reactions of composites. Despite some studies that focused on thermal degradation properties of WF/PVC, a universal and acceptable pyrolysis kinetic model for WF/PVC composites with and without chitosan are not yet available.

The aim of our present work is to firstly investigate the pyrolysis kinetic models of WF/PVC before and after adding chitosan at optimum addition amounts and particle size for its best performance of naturally coupling function according to our previous conclusions using thermogravimetry (TGA). Kinetics parameters of pyrolysis based on two dominant reaction regions, consisting of activation energy, reaction order, and frequency factor, were also studied. This data will be very crucial and useful support for both the design and optimization of reactors and the further utilization of WF/CS/PVC.

EXPERIMENTAL

Raw Materials

PVC (DG-800) with an average degree of polymerization and density of 800 and 1.35 g/cm^3, respectively, was bought from Tianjin Dagu Chemical Ltd. Co., China. Wood flour of *Cunninghamia lanceolata* with particle size of 80 to 100 mesh was provided by Guangzhou Minshan New Material Ltd. Co., China. The flakes of chitosan had a degree of deacetylation, average molecular mass, and particle size of 95%, 820,000, and 180 to 220 mesh, respectively, and were obtained from Golden-shell Biochemical Ltd. Co., China. Other additives, including heat stabilizers, processing aids, and lubricants, were supplied by Yunnan Zhongqian Ltd. Co., China.

Preparation of Composites

WF and CS were pre-dried at 105 °C for 72 h in an oven prior to blending. Both WF (40 phr) and PVC (100 phr) were mixed in a high speed blender (SHR-10A, Zhangjiagang, China) at 1800 rpm for 8 min. Then CS was added into 2 wt% acetic acid solution while stirring at 40 °C for 30 min. After cooling down to room temperature, the solution was sprayed onto the compounds of wood flour and PVC and mixed for 10 min at 85 °C. Other additives, including heat stabilizer (4 phr), processing aids (6 phr), and lubricants (0.8 phr), also were added and mixed at 105 °C for 10 min. Subsequently, the mixture was extruded as a sheet by conical twin-screw extruders (LSE-35, Guangzhou, China) with a screw diameter of 40 mm and length to diameter ratio of 13:1, corresponding to the temperatures of 130, 145, 165, 180, and 178 °C from hopper to die zone; its rotation speed was set at 25 rpm.

Thermal Degradation Properties Measurement

The measurement of thermal degradation properties for WF/PVC and WF/CS/PVC were carried out on a thermogravimetric instrument (TGA 209-F1, Netzsch Co., Germany) to obtain the data about weight loss during the continuous heating. Samples of 10 mg were heated from 30 to 800 °C under the protection of a high purity nitrogen atmosphere at a heating rate of 10 $°C \cdot min^{-1}$.

Pyrolysis Kinetic Model Calculation

The pyrolysis process of samples can be expressed as follows: samples → volatile + solid residue. The decomposition rate of samples is generally described as follows according to the Arrhenius equation (Eq. 1),

$$\frac{d\alpha}{dt} = kf(\alpha) = A\exp(-\frac{E}{RT})f(\alpha) \tag{1}$$

where, $f(\alpha)$ is a characteristic function depending on the reaction mechanism; k is the rate constant of decomposition; A is the frequency factor (s^{-1}); E is the apparent activation energy of decomposition ($J \cdot mol^{-1}$); R is the universal gas constant (8.314 $J \cdot mol^{-1} \cdot K^{-1}$); and T is the absolute temperature, in K. Also, α is the fractional conversion at certain time (s), which can be defined (Eq. 2) as,

$$\alpha = \frac{W_0 - W_t}{W_0 - W_\infty} = \frac{\Delta W_t}{\Delta W_\infty} \tag{2}$$

where, W_0 is the initial weight of sample (g); W_t is the weight of sample at t time (g); W_∞ is the final weight of the sample (g); ΔW_t is the mass loss at t time (g); and ΔW_∞ is the mass loss at the end of the reaction (g).

Under non-isothermal TGA, a constant heating rate ($dT/dt=\beta$) is often used and Eq. 1 becomes Eqs. 3 and 4.

$$\frac{d\alpha}{dt} = \frac{d\alpha}{dt} \cdot \frac{dt}{dT} = kf(\alpha) \cdot \frac{1}{\beta} = A\exp(-\frac{E}{RT})f(\alpha) \cdot \frac{1}{\beta} \tag{3}$$

$$\frac{d\alpha}{f(\alpha)} = \frac{A}{\beta}\exp(-E/RT)dT \tag{4}$$

In this study, the Coats-Redfern integration method was applied to determine the kinetic parameters (Coats and Redfern 1964; Liu *et al*. 2002). The parameter $g(\alpha)$ was defined as shown by Eq. 5:

$$g(\alpha)=\int_0^{\alpha}\frac{d(\alpha)}{f(\alpha)} \tag{5}$$

Equation 6 was formed by combining Eqs. 1 and 5.

$$g(\alpha)=\frac{A}{\beta}\int_{T_0}^{T}(-E/RT)dT \tag{6}$$

Re-arranging and integrating Eq. 4 gives (Eq. 7):

$$\ln[\frac{g(\alpha)}{T^2}]=\ln[\frac{AR}{\beta E}(1-\frac{2RT}{E})]-\frac{E}{RT} \tag{7}$$

The kinetic model *g*(*α*) is an algebraic expression which is usually associated with a physical model for the description of the kinetics in a solid state reaction. The most common forms of *g*(*α*) are listed in Table 1. A suitable model was estimated by the accuracy of linear regression of ln[$g(\alpha)/T^2$] to 1/*T*.

It was known from equation (7) that the term 2R*T*/*E* is much less than 1 for the thermal decomposition of composites. Therefore, ln[$g(\alpha)/T^2$] to 1/*T* should be a line with the slope of *E*/R when the correct *g*(*α*) is matched. Meanwhile, the activation energy (*E*) and frequency factor (*A*) can be calculated through the slope and intercept of the line.

Table 1. Kinetic Model Functions *f*(a) and Corresponding *g*(a) Usually Employed for the Solid State Reactions

Models	$g(\alpha)$	$f(\alpha)$
First-order reaction order (L1)	$-\ln(1-\alpha)$	$1-\alpha$
Second-order reaction order (L2)	$(1-\alpha)^{-1}-1$	$(1-\alpha)^2$
Third-order reaction order (L3)	$((1-\alpha)^{-2}-1)/2$	$(1-\alpha)^3$
Contracting area (R2)	$1-(1-\alpha)^{1/2}$	$2(1-\alpha)^{1/2}$
Contracting volume (R3)	$1-(1-\alpha)^{1/3}$	$3(1-\alpha)^{2/3}$
1-D diffusion (D1)	α^2	$1/2\alpha$
2-D diffusion (D2)	$(1-\alpha)\ln(1-\alpha)+\alpha$	$[-\ln(1-\alpha)]^{-1}$
3-D diffusion-Jander (D3)	$[1-(1-\alpha)^{1/3}]^2$	$3/2(1-\alpha)^{2/3}[1-(1-\alpha)^{1/3}]^{-1}$
Ginstling-Brounshtein (D4)	$(1-2\alpha/3)-(1-\alpha)^{2/3}$	$3/2[(1-\alpha)^{-1/3}-1]^{-1}$

RESULTS AND DISCUSSION

Thermal Degradation Properties Analysis

Figure 1 shows the TG curves of WF/PVC composites without chitosan and WF/PVC/CS with 30 phr chitosan. Two main mass loss processes (220 to 400 °C and 400 to 540 °C) were clearly evident. It was suggested that major pyrolysis of semi-cellulose, cellulose, and chitosan, as well as partial decomposition of lignin occurred, besides the volatilization of hydrogen chloride (HCl) at the first stage (Cardenas and Miranda 2004; Fang *et al*. 2012). Specifically, the amorphous structures of branches were removed from the main chains of hemicelluloses. Long chains of glucose units were broken for cellulose and chitosan. Aromatic rings in lignin appeared to be cross-linked

(Levchik and Wei 2005; Yang *et al*. 2007). The second stage mainly involved thermal cracking of the carbonaceous conjugated polyene sequences in PVC (Diab *et al*. 2011).

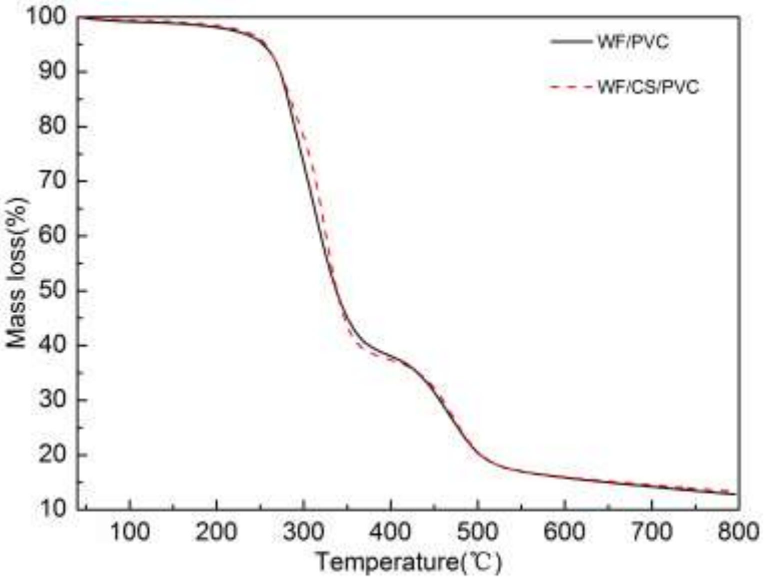

Fig. 1. TG curves of WF/PVC and WF/PVC/CS composites

The observed thermal degradation curve of WF/PVC appeared to be different from that of the WF/PVC/CS in a nitrogen atmosphere. Specifically in Table 2, the temperature at 10% weight loss ($T_{10\%}$) of WF/PVC, which represents the volatilization of water, was almost the same (nearly 273 °C) as WF/PVC/CS due to the constant control of the moisture content of WF and CS in pre-drying process. However, $T_{30\%}$ and $T_{70\%}$ of WF/PVC/CS were prolonged to 312.7 °C and 459.2 °C from 304.8 °C and 455.5 °C of WF/PVC, which demonstrated that the thermal stability of WF/PVC/CS was promoted effectively because the ability of the interfacial interlock was strengthened with the autocatalytic effect of HCl on dehydrochlorination of PVC chains being weaken. Additionally there was a possible acid-base neutralization reaction taking place between HCl and alkaline chitosan. Moreover, the residue content of WF/PVC/CS was also higher than WF/PVC, since the carbon element of CS was brought into the whole compound system.

Table 2. The Data of TG Curve

Groups	$T_{10\%}$/°C	$T_{30\%}$/°C	$T_{70\%}$/°C	Solid residue/%
WF/PVC	272.9	304.8	455.5	12.81
WF/PVC/CS	272.8	312.7	459.2	13.28

$T_{10\%}$, $T_{30\%}$ and $T_{70\%}$ represented temperature at 10 %, 30 % and 70 % weight loss, respectively.

Pyrolysis Kinetic Model Analysis

Based on the analyses above, a two-stage model including two independent thermal degradation processes that occurred in the 240 to 400 °C and 400 to 540 °C temperature ranges is proposed to describe the mass loss kinetics of WF/PVC and WF/CS/PVC. The experimental curves with nine types of models were fitted as shown in

Figs. 2 and 3. The specific data of fitted equations with correlation coefficients (R^2) were listed in Table 3 and Table 4.

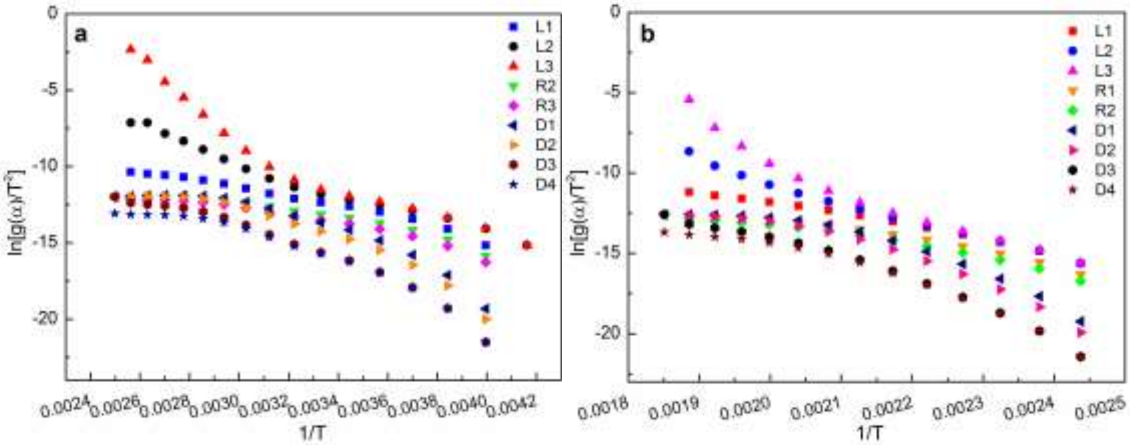

Fig. 2. Models of two thermal degradation processes of WF/PVC composites

As for WF/PVC composites, it was found from Fig. 2a that the function of the first-order reaction order (L1) showed the best extent of linearity. Moreover, it was also noticed in Table 3 that L1 with the fitted equation y =-3133.852x-2.037 and maximum R^2=0.976 implied that the model function of L1 is the best reaction order function for the description of mass loss kinetic for WF/PVC composites without chitosan during the first stage.

Table 3. The Fitted Equations with Correlation Coefficients (R^2) of Two Stages for WF/PVC Composites without Chitosan

Degradation process	Models	Fitted equation	R^2
First stage	L1	y = -3133.852x-2.037	0.976
	L2	y = -4915.692x+5.119	0.971
	L3	y = -7683.704x+15.494	0.915
	R2	y = -2344.295x-5.608	0.905
	R3	y = -2573.443x-5.175	0.937
	D1	y = -4347.427x+0.092	0.857
	D2	y = -5152.316x+2.335	0.912
	D3	y = -5776.033x+3.173	0.952
	D4	y = -5148.128x+0.876	0.916
Second stage	L1	y = -7796.445x+3.762	0.985
	L2	y = -11766.382x+12.968	0.987
	L3	y = -16808.133x+24.631	0.943
	R2	y = -6072.906x-0.922	0.938
	R3	y = -6611.968x-0.078	0.962
	D1	y = -10805.305x+8.523	0.889
	D2	y = -12863.814x+12.582	0.937
	D3	y = -14164.749x+14.158	0.967
	D4	y = -12692.428x+10.748	0.938

As for the second stage, the pyrolysis model curve in Fig. 2b corresponds to the optimum fitted equation of y=-11766.382x+12.968 (L2 model) with R^2=0.987 in Table 3. Nevertheless the other fitted equation: y= -7796.445x+3.762 also achieved a high coefficient of determination value R^2=0.985 (L1 model), which indicated that there were less obvious differences between the L1 and L2 model. This implied that the description of mass loss behaviors for WF/PVC composites without chitosan can be acceptable for both L1 and L2 at the second thermal degradation stage, but L2 was preferred. The reason may be that the two kinetic models for the two temperature ranges take effect together in the intermediate range from the first stage to the second stage (*i.e.*, at the temperatures from the end of the first range to the beginning of the second range).

With respect to the WF/CS/PVC samples examined by nine model functions at two stages, it can be seen in Fig. 3 and Table 4 that the model functions of the second-order reaction order (L2) resulted in maximum coefficients of determination (R^2) of 0.990 and 0.988, corresponding to the following two fitted equations: y = -4917.745x+4.542 and y = -11171.812x +11.844 for both the first and second thermal degradation processes. This demonstrated that the addition of chitosan did alter the pyrolysis behaviors at the two stages.

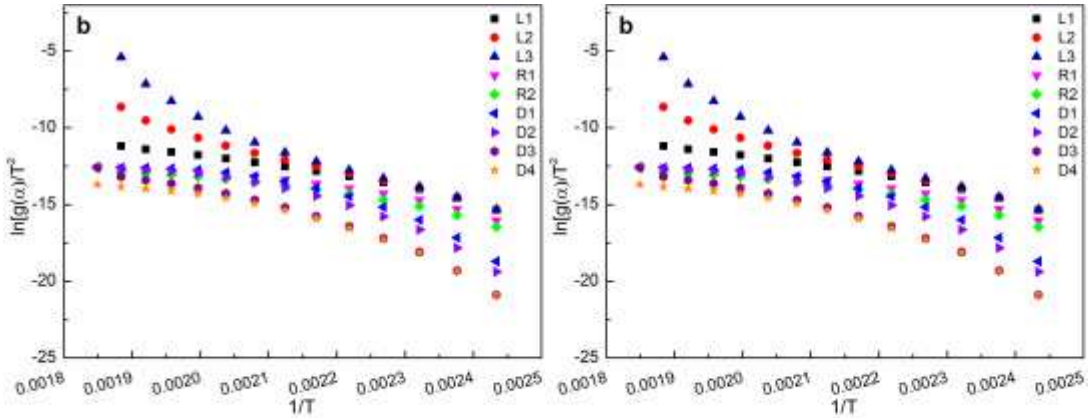

Fig. 3. Models of two thermal degradation processes of WF/CS/PVC composites without chitosan

Table 4. The Fitted Equations with Correlation Coefficients (R^2) of Two Stages for WF/CS/PVC Composites

Degradation process	Models	Fitted equation	R_2
First stage	L1	y = -3073.870x-2.205	0.951
	L2	y = -4917.745x+4.542	0.990
	L3	y = -7271.862x+13.125	0.951
	R2	y = -2318.359x-5.660	0.862
	R3	y = -2538.246x-5.258	0.901
	D1	y = -4329.478x+0.095	0.814
	D2	y = -5147.663x+2.388	0.875
	D3	y = -5707.287x+3.012	0.923
	D4	y = -5105.314x+0.802	0.881
Second stage	L1	y = -7152.500x+2.510	0.975
	L2	y = -11171.812x+11.844	0.988
	L3	y = -16289.481x+23.697	0.949
	R2	y = -5464.158x-2.103	0.920
	R3	y = -6001.928x-1.260	0.948
	D1	y = -9604.247x+6.180	0.863
	D2	y = -11559.114x+10.017	0.916
	D3	y = -12945.604x+11.797	0.956
	D4	y = -11476.211x+8.386	0.921

The kinetic parameters of WF/PVC and WF/CS/PVC, activation energy (*E*) and frequency factor (*A*), calculated from these equations' best linearity, are summarized in Table 5. It was found that the activation energy value obtained from WF/CS/PVC sample (40.89 kJ·mol^{-1}) was greater than the value estimated by WF/PVC (26.05 kJ·mol^{-1}) without chitosan during the first thermal degradation stage. One major explanation was that adding chitosan allowed the bio-polymer coupling agent to improve the interfacial bonding of the PVC resin matrix and wood flour, WF, PVC, and CS, allowing these components to become combined into an integral system, which led to relatively high activation energy. However, the ability to resist thermal degradation for the whole system gradually got weaker when the temperature was over the maximum degradation temperature of pure CS (about 300 °C) (Diab *et al*. 2011), so the activation energy (*E*) was lower for WF/CS/PVC (92.88 kJ·mol^{-1}) than for WF/PVC (97.83 kJ·mol^{-1}). In addition, Table 4 also showed that the frequency factor (*A*) of WF/CS/PVC was much higher than the one of WF/PVC without chitosan. It can be deduced that adding chitosan successfully incorporated into the interfacial bonding system effect. The result of the calculated kinetic parameters for pyrolysis of WF/PVC and WF/CS/PVC correlated well with our previous research for WF/CS/PVC composites (Xu *et al*. 2014b).

According to the kinetic parameters and optimum models, the pyrolysis kinetic equations for WF/PVC and WF/PVC/CS samples at the first thermal degradation stage corresponded to $d\alpha/dt=4.08\times10^{3}\times(1-\alpha)\times\exp(-26050/RT)$ and $d\alpha/dt=2.11\times10^{10}\times(1-\alpha)^{2}\times\exp(-40890/RT)$. At the second thermal degradation stage, they corresponded to $d\alpha/dt=1.11\times10^{7}\times(1-\alpha)^{2}\times\exp(-97830/RT)$ and $d\alpha/dt=1.56\times10^{11}\times(1-\alpha)^{2}\times\exp(-92880/RT)$, respectively.

Table 5. Pyrolysis Kinetic Parameters of Different Group Samples

Groups	Temperature range (°C)	Activation energy (*E*) (kJ·mol^{-1})	Frequency factor (*A*) (s^{-1})
WF/PVC	240 to 400	26.05	4.08×10^{3}
WF/CS/PVC	240 to 400	40.89	2.11×10^{10}
WF/PVC	400 to 540	97.83	1.11×10^{7}
WF/CS/PVC	400 to 540	92.88	1.56×10^{11}

CONCLUSIONS

1. The thermal degradation temperature of WF/PVC composites increased after adding chitosan.
2. The L1 model with the fitted equation $y=-3133.852x-2.037$ and L2 model with fitted equation $y=-11766.382x+12.968$ were the best reaction order functions for the description of mass loss kinetics of WF/PVC at the first and second stages. Two L2 models with fitted equations: $y=-4917.745x+4.542$ and $y=-11171.812x+11.844$, were suitable for the first and second thermal degradation stages of WF/CS/PVC.
3. The pyrolysis kinetic equations for the WF/PVC and WF/CS/PVC samples at the first thermal degradation stage were $d\alpha/dt=4.08\times10^{3}\times(1-\alpha)\times\exp(-26050/RT)$ and $d\alpha/dt=2.11\times10^{10}\times(1-\alpha)^{2}\times\exp(-40890/RT)$, respectively; at the second thermal degradation stage they were $d\alpha/dt=1.11\times10^{7}\times(1-\alpha)^{2}\times\exp(-97830/RT)$ and $d\alpha/dt=1.56\times10^{11}\times(1-\alpha)^{2}\times\exp(-92880/RT)$.

ACKNOWLEDGMENTS

This work was sponsored by the grants of the National Natural Science Funds of China (No. 31160147), the Basic Research on the Application of the Key Project of Yunnan Province (No. 2011FA021), as well as the Scientific Funds of Southwest Forestry University (No. 111419).

REFERENCES CITED

Cardenas, G., and Miranda, S. P. (2004). "FTIR and TGA studies of chitosan composite films," *Journal of the Chilean Chemical Society* 49(4), 291-295.

Cavdar, A. D., Mengeloglu, F., Karakus, K., and Tomak, E. D. (2014). "Effect of chemical modification with maleic, propionic, and succinic anhydrides on some properties of wood flour filled HDPE composites," *BioResources* 9(4), 6490-6503. DOI: 10.15376/biores.9.4.6490-6503

Coats, A. W., and Redfern, J. P. (1964). "Kinetic parameters from thermogravimetric data," *Nature* 201, 68-69.

Czégény, Z., Jakab, E., Bozi, J., and Blazsó, M. (2015). "Pyrolysis of wood-PVC mixtures. Formation of chloromethane from lignocellulosic materials in the presence of PVC," *Journal of Analytical and Applied Pyrolysis* 113, 123-132. DOI:10.1016/j.jaap.2014.11.016

Diab, M. A., El-Sonbati, A. Z., and Bader, D. M. D. (2011). "Thermal stability and degradation of chitosan modified by benzophenone," *Spectrochimica Acta A* 79(5), 1057-1062. DOI: 10.1016/j.saa.2011.04.019

Fabiyi, J. S., McDonald, A. G., and McIlroy, D. (2009). "Wood modification effects on weathering of HDPE-based wood plastic composites," *Journal of Polymers and the Environment* 17(1), 34-48. DOI: 10.1007/s10924-009-0118-y

Fang, Y., Wang, Q., Bai, X., Wang, W., and Cooper, P. A. (2012). "Thermal and burning properties of wood flour poly(vinyl chloride) composite," *Journal of Thermal Analysis and Calorimetry* 109(3), 1577-1585. DOI: 10.1007/s10973-011-2071-y

Jiang, H. H., and Kamdem, D. P. (2004). "Development of poly(vinyl chloride)/wood composites. A literature review," *Journal of Vinyl and Additive Technology* 10(2), 59-69. DOI: 10.1002/vnl.20009

Karayildirim, T., Yanik, J., Yuksel, M., Saglam, M., Vasile, C., and Bockhorn, H. (2006). "The effect of some fillers on PVC degradation," *Journal of Analytical and Applied Pyrolysis* 75(2), 112-119. DOI: 10.1016/j.jaap.2005.04.012

Kositchaiyong, A., Rosarpitak, V., Prapagdee, B., and Sombatsompop, N. (2013). "Molecular characterizations, mechanical properties and anti-algal activities for PVC and wood/PVC composites containing urea- and triazine-based algaecides," *Composites Part B-Engineering* 53, 25-35. DOI: 10.1016/j.compositesb.2013.04.036

Kositchaiyong, A., Rosarpitak, V., Hamada, H., and Sombatsompop, N. (2014). "Anti-fungal performance and mechanical morphological properties of PVC and wood/PVC composites under UV-weathering aging and soil-burial exposure," *International Biodeterioration and Biodegradation* 91, 128-137. DOI: 10.1016/j.ibiod.2014.01.022

Levchik, S. V., and Weil, E. D. (2005). "Overview of the recent literature on flame retardancy and smoke suppression in PVC," *Polymer for Advanced Technologies* 16(10), 707-716. DOI: 10.1002/pat.645

Liu, N. A., Fan, W., Dobashi, R., and Huang, L. (2002). "Kinetic modeling of thermal decomposition of natural cellulosic materials in air atmosphere," *Journal of Analytical and Applied Pyrolysis* 63(2), 303-325. DOI: 10.1016/S0165-2370(01)00161-9

Lu, J. Z., Duan, X. F., Wu, Q. L., and Lian, K. (2008). "Chelating efficiency and thermal, mechanical and decay resistance performances of chitosan copper complex in wood-polymer composites," *Bioresource Technology* 99(13), 5906-5914. DOI: 10.1016/j.biortech.2007.09.086

McNeill, I., Memetea, L., and Cole, W. (1995). "A study of the products of PVC thermal degradation," *Polymer Degradation and Stability* 49(1), 181-191. DOI: 10.1016/0141-3910(95)00064-S

Sain, M., Park, S. H., Suhara, F., and Law, S. (2004). "Flame retardant and mechanical properties of natural fibre-PP composites containing magnesium hydroxide," *Polymer Degradation and Stability* 83(2), 363-367. DOI: 10.1016/S0141-3910(03)00280-5

Segerholm, B. K., Ibach, R. E., and Westin, M. (2012). "Moisture sorption, biological durability, and mechanical performance of WPC containing modified wood and polylactates," *BioResources* 7(4), 4575-4585. DOI: 10.15376/biores.7.4.4575-4585

Snegireva, A. Y., Talalova, V. A., Stepanova, V. V., and Harris, J. N. (2012). "Formal kinetics of polystyrene pyrolysis in non-oxidizing atmosphere," *Thermochimica Acta* 548, 17-26. DOI: 10.1016/j.tca.2012.08.021

Xu, K. M., Li, K. F., Yun, H., Zhong, T. H., and Cao, X. L. (2013). "A comparative study on inhibitory ability for various wood based composites against harmful biological species," *BioResources* 8(4), 5749-5760.

Xu, K., Li, K., Zhong, T., and Xie, C. (2014a). "Interface self-reinforcing ability and antibacterial effect of natural chitosan modified polyvinyl chloride-based wood flour composites," *Journal of Applied Polymer Science* 131(3), DOI: 10.1002/app.39854.

Xu, K. M., Li, K. F., Zhong, T. H., and Xie, C. P. (2014b). "Effects of biopolymer on the thermal and rheological behavior of polyvinyl chloride wood flour composites," *Composites Part B: Engineering* 58(2), 392-399. DOI: 10.1016/j.compositesb.2013.10.056

Yang, H., Yan, R., Chen, H., Lee, D. H., and Zheng, C. (2007). "Characteristics of hemicellulose, cellulose and lignin pyrolysis," *Fuel* 86(12-13), 1781-1788. DOI: 10.1016/j.fuel.2006.12.013

Yue, X. P., Chen, F., and Zhou, X. S. (2011). "Improved interfacial bonding of PVC/wood flour composites by lignin amine modification," *BioResources* 6(2), 2022-2034.

Article submitted: February 2, 2015; Peer review completed: June 9, 2015; Revised version received and accepted: June 12, 2015; Published: June 23, 2015.
DOI: 10.15376/biores.10.3.4903-4912